

Carbon nanotube-Si diode as a detector of mid-infrared illumination

Pang-Leen Ong,¹ William B. Euler,² and Igor A. Levitsky^{1,2,a)}

¹Emitech, Inc., Fall River, Massachusetts 02720, USA

²Department of Chemistry, University of Rhode Island, Kingston, Rhode Island 02881, USA

(Received 14 November 2009; accepted 2 December 2009; published online 19 January 2010)

We report a room temperature mid-infrared photodetector based on a carbon nanotube-silicon heterojunction nanostructure. The observed mid-infrared band (8–12 μm) in the photocurrent spectrum is consistent with the estimated band gap energy of semiconducting multiwall nanotubes (15 to 30 nm diameter). The fast response time (16 ms) and small temperature change ($\sim 10^{-8}$ K) upon infrared light suggest that the photocurrent response is not due to bolometric effect. We determined that the primary mechanism of the photocurrent in this spectral range is associated with photon absorption of semiconducting multiwalled carbon nanotubes followed by charge separation at the interface, their transport, and collection at the external electrodes.

© 2010 American Institute of Physics. [doi:10.1063/1.3279141]

For the last decade, the photoconductivity of carbon nanotubes (CNTs) has attracted great interest due to possible applications of their unique optoelectronic properties for the development of novel photosensitive nanomaterials for photovoltaics,^{1–8} photodetectors,^{9–12} and bolometers.^{13–15} Most of these studies were related to CNT photoconductive response upon exposure to visible and near infrared light of individual CNTs, bundles, or films (freely suspended^{10,15} or deposited on an insulating substrate^{11,12,14}), CNT-conjugated polymer composites,^{2–4,12,14} and CNT-semiconductor interfaces,^{6–9} which was motivated by the benefits for solar energy conversion.

Very recently, several groups reported hybrid photovoltaics based on a CNT *n*-type Si heterojunction.^{6–9} A major advantage of such an approach is the combination of charge separation at the CNT-*n*Si interface along with charge transport and collection through the CNT network. In a study of photoresponse of CNT-*n*Si diode to mid-IR, Tzolov *et al.*⁹ observed a band (maximum at 0.45 eV or 2.8 μm) in the mid-IR spectral range in the photocurrent spectrum, which was interpreted as the interband transitions for semiconducting multiwalled nanotubes (MWNTs). The device structure was a vertical array of chemical vapor deposition (CVD) grown MWNTs in a nanoporous alumina template on a silicon substrate. There is a possibility that incomplete removal of the alumina matrix resulted in several undesired effects for the diode performances, e.g., a barrier layer between nanotubes and Si or surface traps in alumina. In addition, the response time detected was in the range of one second, which indicated an influence of a thermal effect, either complex interaction of MWNTs with alumina/Si or due to oxygen desorption.¹¹

In this letter, we report that MWNT-*n*Si diode prepared by a simple spray deposition technique demonstrates photoconductive response in the mid-IR region in nonbiased mode. As distinct from the previous study,⁹ such an approach provides a direct contact of MWNTs with *n*-type Si, allowing study of control samples [single walled nanotubes (SWNT)-*n*Si] where no IR response in the same spectral range was detected as compared with MWNT-*n*Si structure.

In addition, the device exhibited a fast response time, which cannot be associated with a bolometric effect or to oxygen desorption.

For this study, purified MWNT (15–30 nm diameter, acid treated from Nanocs, Inc.) and purified semiconducting SWNTs (7,6 major chirality obtained from SouthWest Nano Technologies, Inc.) were used. The sample preparation procedures are described elsewhere.⁸ Briefly, the diodes were fabricated by spraying MWNT/SWNT through a 5 \times 5 mm² window (active area) on a *n*-type Si (100 orientation, $\rho=0.01 \Omega \text{ cm}$) surface. Prior to spraying, nanotubes were centrifuged (6500 rpm) and the sediment collected after decantation was redispersed by sonication in dichlorobenzene. A layer of Cr/Au (20 nm/150 nm) was sputtered on the back side of the Si wafer to form an Ohmic back contact with Si. The top contact to the MWNT/SWNT film was made by a thin strip of silver paint (1 \times 5 mm²) over the MWNT/SWNT film. Time response and current-voltage (*I*-*V*) characteristics were detected using a Keithley 238 controlled by LabVIEW software. Photocurrent spectra measurements at zero bias were carried out using a Bruker Tensor 27 Fourier transform infrared (FTIR) spectrometer equipped with an analog/digital converter module under IR Globar source illumination. Amplitude-frequency dependences were detected with a digital oscilloscope (HP 54502A) synchronized with a chopper (frequency range ~ 4 –400 Hz) placed between the sample and IR source.

SEM image of the MWNT-*n*Si diode cross-section is presented in Fig. 1(a), where a direct contact can be seen between the MWNTs and the *n*-type Si surface. Figure 1(b) shows the *I*-*V* characteristics of the device under dark and under IR illumination. A long pass germanium filter (LF) was used to filter photon energy higher than 0.6 eV (cutoff wavelength is 2000 nm) in order to avoid any response from the Si band edge. There is a clear indication of an existence of a short circuit current ($I_{\text{SC}}=1.5 \times 10^{-4} \text{ mA/cm}^2$) and open circuit voltage ($V_{\text{OC}}=1.1 \text{ mV}$) under low intensity IR light (15 mW/cm²) based on the shift of the *I*-*V* curves, shown on a semilog scale. Thus, the device can function in the photovoltaic regime without any external bias. The photocurrent spectrum [Fig. 2(a) blue curve] of the same device without LF reveals an intense band (onset at 1.1 eV) corre-

^{a)}Electronic mail: ilevitsky@chm.uri.edu.

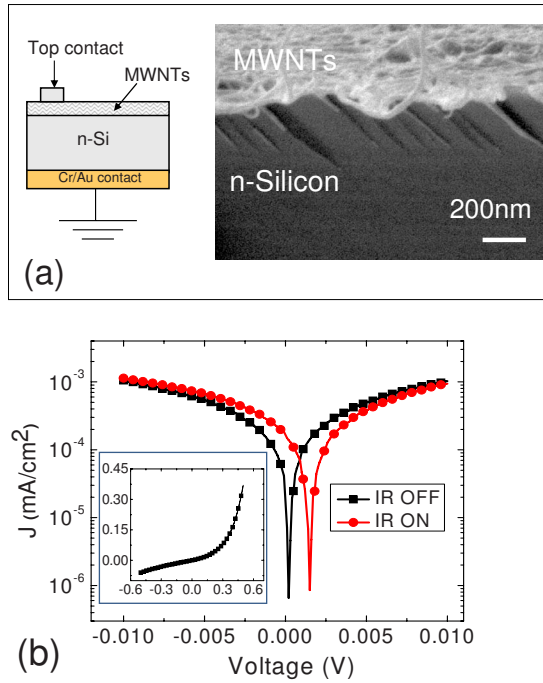


FIG. 1. (Color online) (a) Schematic illustration of MWNT-*n*Si heterojunction device and a SEM image of the MWNT-*n*Si interface. (b) Current-voltage (*I*-*V*) plot of MWNT-*n*Si devices showing the photovoltaic response under low intensity IR light (15 mW/cm²). Inset: dark current-voltage characteristics on a linear scale; x-axis is V and y-axis is mA/cm².

sponding to Si absorption and a low intensity band in mid-IR (centered at 0.15 eV), which can be assigned to interband transitions in semiconducting MWNTs. Introducing the LF [Fig. 2(a) red curve] completely suppresses the Si band, but the mid-IR band feature remains unchanged. Finally, to ensure that this spectral feature is associated with the MWNT-*n*Si interface, a control sample (SWNT-*n*Si diode) was measured and the mid-IR band was not observed in the photocurrent spectrum [Fig. 2(a) black curve]. It is assumed that there is no band gap in mid-IR range for semiconducting SWNTs of smaller diameter (~ 0.9 nm). The origin of the mid-IR photocurrent band can be associated with electron transition through the band gap of semiconducting MWNTs with diameters in the range of 15–30 nm. The band gap of the MWNTs is in the range of 0.025 to 0.05 eV based on the formula, $E_G = (2 \times \gamma \times a_{C-C})/d_t$,¹⁶ where d_t is the diameter of the nanotubes, γ is 2.77 eV, and a_{C-C} (0.1421 nm) is the nearest neighbor C–C distance. The calculated band gap is in a good agreement with the value of 0.025 eV obtained from a Tauc plot¹⁷ [Fig. 2(a), inset].

An alternative explanation of the IR photoresponse could be related to photoelectric emission, similar to a Schottky barrier type photodiode,¹⁸ or due to heating effect (bolometric response). To explore these possibilities, we employed the band diagram of MWNT-*n*Si heterojunction based on Anderson model [Fig. 2(b)] which was constructed using the MWNT conduction band (E_C) of 4.8 eV,¹⁹ MWNT band gap of 0.025 eV, and assuming that Fermi level is located in the middle of the band gap. In the case of photoelectric emission, in order for photogenerated electrons to overcome the band gap and barrier height $\sim (0.05 + 0.7)$ eV the photon energy should be in the same range, which is inconsistent with the spectral position of the observed mid-IR band (onset at 0.025 eV, maximum at 0.15 eV).

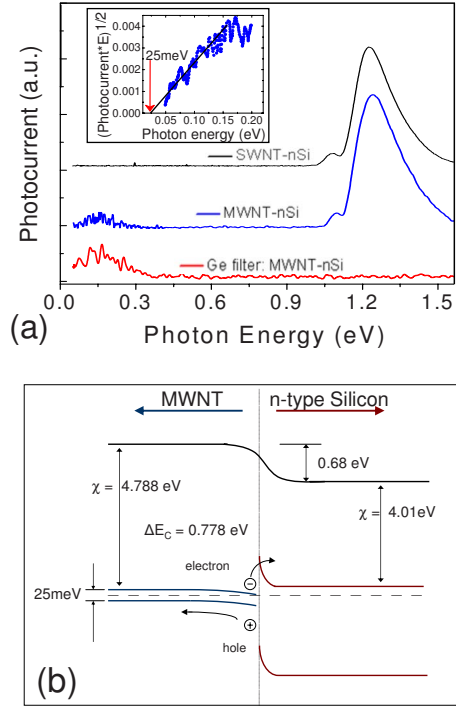


FIG. 2. (Color online) (a) Normalized photocurrent spectra (based on the intensity of IR Global source) of the MWNT-*n*Si devices with (red curve) and without (blue curve) LF and control SWNT-*n*Si device (black curve). Inset: Tauc plot data at 300 K, which is used to determine the band gap of the CNTs. The band gap, E_G (0.025 eV) of the MWNTs (15–30 nm diameters) is obtained via extrapolation to the zero crossing of the E -axis. It is known that E_G can be determined by extrapolation of the Tauc plot $\{[\alpha(\omega)E]^{1/2} \sim (E - E_G)\}$, where $\alpha(\omega)$ is the absorption) to the zero crossing of the E axis for the absorption band edge of semiconductors. (b) Energy band diagram of MWNT-*n*Si heterojunction based on Anderson model. Electron affinity, χ and conduction band offset, ΔE_C for MWNTs and *n*Si are shown in the schematic.

The heating effect may be more plausible as an explanation. However, at least three arguments can be presented against such an interpretation. First, an estimate of the temperature change can be made based on the expression $\Delta T = \alpha J / G_p$, where α is the absorption coefficient, J is the IR power and G_p is the thermal conductivity. Taking $\alpha \sim 0.5$ in the range of 0.1–0.3 eV (determined by IR absorbance of the same thickness of MWNT sprayed on KBr); $J = 3.5$ mW; and G_p value ~ 100 W/mK, which is an average between the thermal conductivity of Si (~ 150 W/mK) and MWNT [~ 50 W/mK (Ref. 20)], the temperature change is diminishingly small with a value of $\Delta T \sim 10^{-8}$ K. Thus, the corresponding thermal energy, $k_B \Delta T \sim 10^{-13}$ eV $\ll E_G$, cannot provide the energy required for electron transition to the conducting band or to overcome the barrier height of 0.78 eV. Second, it is very unlikely that IR heating (negligible in our case) could induce the photovoltaic effect as observed experimentally [Fig. 1(b)]. Usually heating affects the shape of an *I*-*V* curve, leaving the curve crossing of the (0,0) point unchanged. Third, the measured characteristic time from the time trace (with resolution of 10 ms) [Fig. 3(a)] and more accurately from the amplitude-frequency characteristics [Fig. 3(b)] with LF was $\tau = 16$ ms. According to the expression for bolometric response time, $\tau = C/G$ (where C is thermal capacitance and G is the thermal conductance), the response time τ , is estimated ~ 300 ms based on the sample size, thermal capacitance of MWNT, and Si (~ 700 J/kg K for

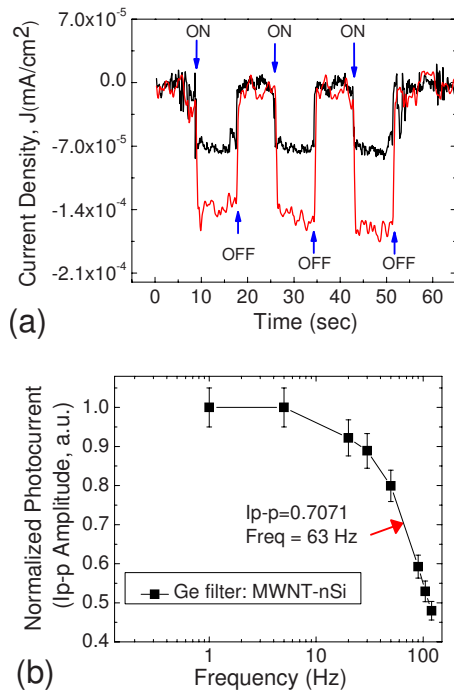


FIG. 3. (Color online) (a) Time traces of photocurrent from MWNT-*n*Si devices (sonication only: black curve, sonication and centrifugation followed by sediment extraction: red curve) under IR illumination with LF. The nanotubes deposited by spraying from the sediment fraction showed $\sim 50\%$ increase in the photocurrent response with respect to the samples without centrifugation. (b) Normalized photocurrent (amplitude of peak to peak current) as a function of frequency. The characteristic time of MWNT-*n*Si photodiode is ~ 16 ms (at ~ 63 Hz) at peak to peak amplitude of 70.7% (3 dB reduction of photocurrent response).

both materials) and Si density (2300 kg/m^3). The discrepancy between the estimated and experimental values of more than an order of magnitude strongly supports the notion that the response time is not a result of diode heating. The characteristic time of 16 ms is significantly shorter than the response time of one second reported by Tzolov *et al.*⁹ which could be explained by the direct contact of MWNTs with Si in the absence of the alumina matrix. Furthermore, as distinct from the previous study,⁹ our diode has no top Au contact. This indicates that the MWNT film serves not only as IR absorber but also as a charge transporter and collector supplying photocarriers to the external electrode (lateral strip of silver). Thus, the characteristic time is mainly defined by carrier diffusion in the lateral direction to the silver electrode.

The mechanism of the IR photocurrent is related to the IR absorption in semiconducting MWNTs, exciton generation and their dissociation on photoelectrons and photoholes at the nanotube-Si interface, followed by charge transport and collection at the external electrodes. We suggest that the separated photoholes at the MWNT-*n*Si interface diffuse from the depleted region to the external top electrode through the nanotube network, while photoelectrons accumu-

late at the interfacial area [see band diagram, Fig. 2(b)] polarizing the interface and partially tunneling through the barrier to the Si component, followed by charge transport and collection at the back electrode. The device responsivity was estimated as $\sim 100 \mu\text{A/W}$ without applying external bias. Note that no optimization schemes were undertaken in this study.

In conclusion, we demonstrated that heterojunction structure fabricated by MWNT spray deposition on *n*-type Si is capable of detecting mid-IR in the range of 8–12 μm without external bias. The primary mechanism of photocurrent is photon absorption of semiconducting MWNTs followed by charge separation at the interface, their transport and collection at the external electrodes. The bolometric response of the diode can be neglected because of extremely low temperature change ($\sim 10^{-8}$ K) and the short response time (16 ms), which is inconsistent with a heating process. The tunable spectral response where the band gap depends on the nanotube diameter, high carrier mobility, simple wet deposition, and scalability makes such nanostructures very attractive for the room temperature IR detection.

This work is supported by the U.S. Government (Army). We thank Dr. Song Youngsik for the SEM images.

- ¹J. Geng and T. Zeng, *J. Am. Chem. Soc.* **128**, 16827 (2006).
- ²B. J. Landi, R. P. Raffaele, S. L. Castro, and S. G. Bailey, *Prog. Photovoltaics Res. Appl.* **13**, 165 (2005).
- ³H. Ago, K. Petritsch, M. S. P. Shaffer, A. H. Windle, and R. H. Friend, *Adv. Mater.* **11**, 1281 (1999).
- ⁴E. Kymakis, E. Koudoumas, I. Franghiadakis, and G. A. Amaratinga, *J. Phys. D: Appl. Phys.* **39**, 1058 (2006).
- ⁵J. van de Lagemaat, T. M. Barnes, G. Rumbles, S. E. Shaheen, T. J. Coutts, C. Weeks, I. Levitsky, J. Peltola, and P. Glatkowski, *Appl. Phys. Lett.* **88**, 233503 (2006).
- ⁶Z. Li, V. P. Kunets, V. Saini, Y. Xu, E. Dervishi, G. J. Salamo, A. R. Biris, and A. S. Biris, *Appl. Phys. Lett.* **93**, 243117 (2008).
- ⁷Y. Jia, J. Wei, K. Wang, A. Cao, Q. Shu, X. Gui, Y. Zhu, D. Zhuang, G. Zhang, B. Ma, L. Wang, W. Liu, Z. Wang, J. Luo, and D. Wu, *Adv. Mater.* **20**, 4594 (2008).
- ⁸P.-L. Ong, W. B. Euler, and I. A. Levitsky, "Carbon Nanotube-Si Diode as a dDetector of Mid-IR Illumination," (unpublished).
- ⁹M. B. Tzolov, T.-F. Juo, A. Yin, D. A. Straus, and J. M. Xu, *J. Phys. Chem. C* **111**, 5800 (2007).
- ¹⁰M. Freitag, Y. Martin, J. A. Mishewich, R. Martel, and P. Avouris, *Nano Lett.* **3**, 1067 (2003).
- ¹¹I. A. Levitsky and W. B. Euler, *Appl. Phys. Lett.* **83**, 1857 (2003).
- ¹²B. Pradhan, K. Setyowati, H. Liu, D. H. Waldeck, and J. Chen, *Nano Lett.* **8**, 1142 (2008).
- ¹³M. E. Itkis, F. Borondics, A. Yu, and C. J. Haddon, *Science* **312**, 413 (2006).
- ¹⁴A. E. Aliev, *Infrared Phys. Technol.* **51**, 541 (2008).
- ¹⁵R. Lu, Z. Li, G. Xu, and J. Z. Wu, *Appl. Phys. Lett.* **94**, 163110 (2009).
- ¹⁶R. Saito, G. Dresselhaus, and M. S. Dresselhaus, *Physical Properties of Carbon Nanotubes* (Imperial College Press, London, 1999).
- ¹⁷J. Tauc, *Amorphous and Liquid Semiconductors* (Plenum, New York, 1974).
- ¹⁸A. Rogalski, *Infrared Detectors* (Gordon & Breach, Amsterdam, 2000).
- ¹⁹J. Zhao, J. Han, and J. P. Lu, *Phys. Rev. B* **65**, 193401 (2002).
- ²⁰A. E. Aliev, C. Guthy, M. Zhang, A. A. Zakhidov, J. E. Fisher, and R. H. Baughman, MRS Symposium Proc. No. 963E, 0963-Q16-02 (2006).